cluded. In view of the presence of intense IR absorption bands of OH groups, it is obvious that the amount of strongly chemisorbed water cannot be significant. If strong interactions were to occur between the OH groups and the water molecules, the resolution of the corresponding vibrations would be reduced and they would shift toward lower wavenumbers.[13]

The ^{31}P MAS NMR spectrum of n-DPA-VPI-5 (not shown) contains three signals with chemical shifts of −23.3, −27.2, and −33.1 ppm in the intensity ratio 1:1:1. The ^{27}Al MAS NMR spectrum (see Figure 6) shows the presence of 4-coordinated AlO_4 and 6-coordinated AlO_6 environments at 41.6 and ca. −15 ppm, respectively. The similarity of the ^{31}P and ^{27}Al MAS spectra of n-DPA-VPI-5 and TBA-VPI-5 suggests that the deficiency of phosphorus atoms on the three kinds of crystallographically inequivalent P sites in n-DPA-VPI-5 is random and that the distortion of Al environments due to this deficiency is not reflected in the ^{27}Al MAS NMR spectrum.

After calcination of n-DPA-VPI-5 at 200 °C for 6 h and followed by rehydration of the calcined sample, both ^{31}P and ^{27}Al MAS NMR spectra of it are significantly changed (Figures 6 and 7) indicating the occurrence of a structural transformation. A deconvolution of the ^{31}P spectrum reveals the presence of five peaks at −22.6, −25.7, −26.9, −29.1, and −31.1 ppm in the intensity ratio 1:1:1:1:4.5, while the ^{27}Al spectrum of hydrated calcined n-DPA-VPI-5 shows the presence of 4- and 6-coordinate Al in the intensity ratio 2:1. Because VPI-5 contains 6-coordinate *framework* Al, it is difficult to know whether or not the 6-coordinate Al atoms observed in the ^{27}Al spectrum of the rehydrated calcined sample belong to the framework. We have therefore

investigated the effect of water upon the chemical environments of P and Al atoms in calcined n-DPA-VPI-5: the ^{31}P spectrum of a sample carefully dehydrated at 200 °C under vacuum is poorly resolved, and the relative intensities of the signals are altered. The ^{31}P spectrum, particularly the relative intensities of the peaks, depends upon calcination conditions and the hydration state of the calcined sample. The ^{27}Al spectrum of an anhydrous calcined sample shows a significant decrease in the intensity of the octahedral aluminum signal and a small amount of Al species at ca. 5.5 ppm.

Adsorption of N_2 on calcined VPI-5 gives the surface area to be ca. 117 m^2/g, corresponding to 3 N_2 molecules/unit cell of VPI-5. This indicates that the pores are almost completely blocked by the extraframework species produced during calcination.

Several groups of researchers have suggested that the reason for the irreversible phase transformation in VPI-5 may be the presence of impurities.[3,14] Derouane et al.[3] claim that such impurities can be removed with hot ethanol. Following their procedures precisely, we washed our n-DPA-VPI-5 with hot absolute ethanol at 60 °C for 1 h and calcined the washed sample at 200 °C for 1.5 h. However, XRD showed that the washing does not prevent the onset of structural transformation.

(14) Vogt, E. T. C.; Richardson, J. E., Jr. *J. Solid State Chem.* **1990**, *87*, 469.

Structural Determination of Supported V₂O₅–WO₃/TiO₂ Catalysts by In Situ Raman Spectroscopy and X-ray Photoelectron Spectroscopy

Michael A. Vuurman,[†] Israel E. Wachs,*

Zettlemoyer Center for Surface Studies, and Department of Chemical Engineering, Lehigh University, Bethlehem, Pennsylvania 18015

and Andrew M. Hirt

Materials Research Laboratories, Inc., 720 King Georges Post Road, Fords, New Jersey 08863
(Received: December 3, 1990)

A series of supported V₂O₅/TiO₂, WO₃/TiO₂ and V₂O₅–WO₃/TiO₂ samples have been characterized by means of Raman spectroscopy under ambient as well as in situ dehydrated conditions and by X-ray photoelectron spectroscopy. Under ambient conditions two different hydrated surface vanadia species and crystalline V₂O₅ have been identified in V₂O₅/TiO₂ as a function of surface coverage. Under dehydrated conditions two types of surface vanadium oxide species are found in V₂O₅/TiO₂ samples: a highly distorted vanadium oxide species and a moderately distorted vanadium oxide species, and their relative concentration is a function of the vanadia surface coverage. Under ambient conditions tetrahedrally coordinated surface tungsten oxide species, octahedrally coordinated surface polytungstate species, and crystalline WO₃ are observed in WO₃/TiO₂ samples as a function of surface coverage. Dehydration converts all the two-dimensional tungsten oxide species into a highly distorted octahedrally coordinated structure. The molecular structures of the V₂O₅–WO₃/TiO₂ mixed samples are not influenced by the sequence of impregnation of the starting materials. Under ambient conditions and low vanadia coverage, the hydrated surface vanadium oxide species undergo a structural change due to the acidic nature of tungsten oxide species. Crystalline V₂O₅ and crystalline WO₃ are not influenced by the presence of the other metal oxide. Under dehydrated conditions, both the highly distorted surface vanadium oxide species and the octahedrally coordinated surface tungsten oxide species do not appear to be influenced by each other at all loadings. The only influence observed in this study is that the moderately distorted vanadium oxide species becomes more abundant in the presence of tungsten oxide.

Introduction

Interest in air quality and emission control has resulted in considerable research dealing with the selective reduction of nitrogen oxides.[1] Commercial DeNOₓ catalysts contain V₂O₅–

WO₃/TiO₂. These catalysts are less active than the V₂O₅/TiO₂ catalyst for catalyzing the NOₓ + NH₃ + O₂ reaction but have an excellent thermal stability and a lower oxidation activity for the conversion of SO₂ to SO₃.[2] At this moment, very little

[†]On leave from Anorganisch Chemisch Laboratorium, Universiteit van Amsterdam, Nieuwe Achtergracht 166, 1018 WV Amsterdam, The Netherlands.

(1) Bosch, H.; Janssen, F. *Cat. Today* **1988**, *2*, 369.
(2) Imanari, M.; Watanabe, Y.; Matsuda, S.; Nakajima. *Proceedings of the 7th Congress on Catalysis*; Seiyama, T., Tanabe, K., Eds.; Elsevier: Amsterdam, 1981; p 841.

information is available about the molecular structure of this supported mixed oxide system. Sutsuma et al. investigated the molecular structure of bulk V_2O_5–WO_3 catalysts by means of secondary ion mass spectroscopy, IR spectroscopy of adsorbed NH_3, temperature-programmed desorption, NO–NH_3 rectangular pulse technique, electron spin resonance, X-ray diffraction, and X-ray photoelectron spectroscopy. It was concluded that V_2O_5 and WO_3 are not well mixed in the bulk of the catalyst, but are well-mixed in the surface of the catalyst.[3] Mahipal Reddy et al. studied the influence of MoO_3 and WO_3 on the dispersion of V_2O_5 in vanadia–silica catalysts by using low-temperature oxygen chemisorption, ^{1}H NMR, X-ray diffraction, and ESR. The presence of molybdenum was found to increase the dispersion while the tungsten oxide was found to decrease the dispersion of the vanadium oxide on silica.[4] No characterization studies have been reported for the V_2O_5–WO_3/TiO_2 system to date.

The supported V_2O_5/TiO_2 system has received much attention in the literature because of its superior catalytic activity in the selective oxidation of hydrocarbons.[5] Techniques which have provided direct structural information about the V_2O_5/TiO_2 system under ambient and dehydrated conditions are Raman spectroscopy,[6-16] X-ray absorption spectroscopy (EXAFS, XANES),[17,18] solid-state [51]V NMR spectroscopy,[19] and FTIR spectroscopy.[11,20-22] These studies have revealed that the molecular structure of the supported vanadium oxide phase on titania is different from bulk V_2O_5 and is dependent upon the vanadium oxide loading, surface hydration, surface impurities, and calcination temperature. It has been concluded that under ambient conditions the vanadium oxide forms a two-dimensional overlayer in which more than one vanadium oxide species can be present. At low loading metavanadate species are primarily observed and at higher loadings decavanadate species are primarily present in the hydrated V_2O_5/TiO_2 samples. Under dehydrated conditions two different surface vanadium oxide species are found on the titania surface which possess tetrahedral coordination. One is highly distorted and is observed at all vanadium oxide loadings and the second species is moderately distorted and becomes more pronounced at higher vanadium oxide

loadings. The highly distorted vanadium oxide has been identified as a vanadate species possessing one terminal V=O bond and three bridging V—O—Ti bonds.[10,11,15,19a] For the moderately distorted vanadium oxide species, a polymeric structure[10] or a dioxo polymeric structure has been proposed.[11,15]

The supported WO_3/TiO_2 system has received very little attention in the literature. Characterization of a 7% WO_3/TiO_2 sample by Raman spectroscopy revealed that a two-dimensional overlayer of tungsten oxide is also formed on the titania surface under ambient conditions[6,23,24] and that in situ dehydration drastically changed the tungsten oxide structure.[6,23] No precise information, however, is provided in the literature about the molecular structure of the surface tungsten oxide phase under hydrated and dehydrated conditions.

The purpose of the present study is to determine the molecular structure of supported V_2O_5–WO_3/TiO_2 catalysts and the influence of the mixed oxide system on the vanadium and tungsten structures. Therefore, we have studied the V_2O_5/TiO_2, WO_3/TiO_2, and V_2O_5–WO_3/TiO_2 systems with Raman spectroscopy under ambient and in situ dehydrated conditions as a function of metal oxide loadings. XPS data were also obtained to examine the influence of the mixed oxide system on the dispersion of vanadium and tungsten on the titania surface.

Experimental Section

Sample Preparation. All the samples were prepared by the incipient wetness method on titania (Degussa p-25, 66% anatase, 34% rutile; 55 m²/g). The vanadium oxide catalysts were prepared by impregnation with a solution of $VO(OC_2H_5)_3$ in ethanol. The samples were subsequently dried at room temperature and at 110 °C overnight and calcined in dry air at 450 °C for 2 h. The supported tungsten oxide catalysts were prepared by dissolving ammonium metatungstate ((NH_4)$_6H_2W_{12}O_{40}$) in water and impregnating the TiO_2 support. The samples were then dried at room temperature followed by drying at 110 °C overnight and calcination at 450 °C for 2 h. The V_2O_5–WO_3/TiO_2 mixed oxide catalysts were prepared by a two-step impregnation procedure. First the titania was impregnated with a solution of $VO(OC_2H_5)_3$ in ethanol and dried and calcined as above. Then the tungsten oxide was introduced by impregnation with an aqueous solution of ammonium metatungstate. These mixed samples were subsequently dried at room temperature and at 110 °C overnight and calcined at 450 °C for 2 h in dry air. Another set of V_2O_5–WO_3/TiO_2 mixed oxide catalysts was prepared starting with the impregnation and calcination of the ammonium metatungstate solution as described above. The vanadium oxide was then added by impregnation with a $VO(OC_3H_5)_3$ solution in methanol. Due to the air- and moisture-sensitive nature of this alkoxide precursor, the second impregnation and subsequent drying at room temperature and heating at 350 °C were performed under a nitrogen atmosphere. These mixed oxide samples were finally calcined in dry air at 450 °C for 2 h.

Raman Studies. Two Raman spectrometers were used in this study. Both consisted of a Triplemate spectrometer (Spex, Model 1877) coupled to an optical multichannel analyzer (Princeton Applied Research model 1463) equipped with an intensified photodiode array detector (cooled to −35 °C). One of the Raman spectrometers was used for obtaining the Raman spectra under ambient conditions. The sample was pressed onto KBr and spun at 2000 rpm. The other spectrometer was equipped with an in situ cell in which the temperature and gaseous conditions were controlled. Ultrahigh purity, hydrocarbon-free oxygen (Linde Gas) was purged through the cell. In situ Raman spectra were recorded from stationary samples pressed into self-supporting wafers (no KBr). In a typical experiment, the sample was heated to 450 °C in ∼20 min and held for 30 min. Then the sample was cooled down to 80 °C in ∼1 h. At this temperature the in situ Raman spectrum was recorded. Additional details about the in situ cell

(3) Satsuma, A.; Hattori, A.; Mizutani, K.; Furuta, A.; Miyamoto, A.; Hattori, T.; Murakami, Y. *J. Phys. Chem.* **1988**, *92*, 6052.

(4) Mahipal Reddy, B.; Narsimha, K.; Kanta Rao, P.; Mastikhin, V. M. *J. Catal.* **1989**, *118*, 22.

(5) See, for example: (a) Wachs, I. E.; Saleh, R.; Chan, S. S. *Appl. Catal.* **1985**, *15*, 339. (b) Wainwright, M. S.; Foster, N. R. *Catal. Rev.* **1979**, *19*, 211. (c) Bond, G. C.; Bruckman, K. *Faraday Disc. Chem. Soc.* **1981**, *72*, 235. (d) Gasior, M.; Gasior, I.; Grzybowska, B. *Appl. Catal.* **1984**, *10*, 87. (e) Vanhove, D.; Blanchard, M. *Bull. Soc. Chim. Fr.* **1971**, 3291.

(6) Chan, S. S.; Wachs, I. E.; Murrell, L. L.; Wang, L.; Hall, W. K. *J. Phys. Chem.* **1984**, *88*, 5831.

(7) Wachs, I. E.; Chan, S. S.; Saleh, R. Y. *J. Catal.* **1985**, *91*, 366.

(8) (a) Saleh, R. Y.; Wachs, I. E.; Chan, S. S.; Cherisch, C. C. *J. Catal.* **1986**, *98*, 102. (b) Wachs, I. E.; Hardcastle, F. D.; Chan, S. S. *Proc. Mat. Res. Soc. Sym. Proc.* **1988**, *111*, 353. (c) Hardcastle, F. D.; Wachs, I. E. *Proc. 9th Intern. Congr. Catal.* **1988**, *3*, 1449.

(9) Roozeboom, F.; Mittelmeijer-Hazeleger, M. C.; Moulijn, J. A.; Medema, J.; De Beer, V. H. J.; Gellings, P. J. *J. Phys. Chem.* **1980**, *84*, 2783.

(10) Went, G. T.; Ted Oyama, S.; Bell, A. T. *J. Phys. Chem.* **1990**, *94*, 4240.

(11) Cristiani, C.; Forzatti, P.; Busca, G. *J. Catal.* **1989**, *116*, 586.

(12) Wachs, I. E.; Jehng, J. M.; Hardcastle, F. D. *Solid State Ionics* **1989**, *32*, 904.

(13) Miyata, H.; Fujii, K.; Ono, T. *J. Chem. Soc., Faraday Trans. 1* **1988**, *84*, 3121.

(14) Yoshima, S.; Tanaka, T.; Nishimura, Y.; Mizutani, H.; Funabiki, T. *Proceedings 9th International Congres on Catalysis* **1988**, *3*, 1473.

(15) Wachs, I. E. *J. Catal.* **1990**, *124*, 570.

(16) Deo, G.; Wachs, I. E. *J. Phys. Chem.* **1991**, *95*, 5889.

(17) Kozlowski, R.; Pettifer, R. F.; Thomas, J. M. *J. Phys. Chem.* **1983**, *87*, 5176.

(18) Haber, J.; Kozlowska, A.; Kozlowski, R. *J. Catal.* **1986**, *102*, 52.

(19) (a) Eckert, H.; Wachs, I. E. *J. Phys. Chem.* **1989**, *93*, 6796. (b) Eckert, H.; Deo, G.; Wachs, I. E.; Hirt, A. M. *Colloid Surf.* **1990**, *45*, 347. (c) Eckert, H.; Wachs, I. E. *Mat. Res. Soc. Symp. Proc.* **1988**, *111*, 459.

(20) Miyata, H.; Fujii, K.; Ono, T.; Kubokawa, Y.; Ohno, T.; Hatayama, F. *J. Chem. Soc., Faraday Trans. 1* **1987**, *83*, 675.

(21) Busca, G.; Centi, G.; Marchetti, L.; Trifiro, F. *Langmuir* **1986**, *2*, 568; **1986**, *2*, 557.

(22) Brjorklund, R. B.; Odenbrand, C. U. I.; Brandin, J. G. M.; Andersson, L. A. H.; Liedberg, B. *J. Catal.* **1989**, *119*, 187.

(23) Wachs, I. E.; Hardcastle, F. D.; Chan, S. S. *Spectroscopy* **1986**, *1*, 30.

(24) Bond, G. C.; Flamertz, S.; van Wijk, L. *Cat. Today* **1987**, *1*, 229.
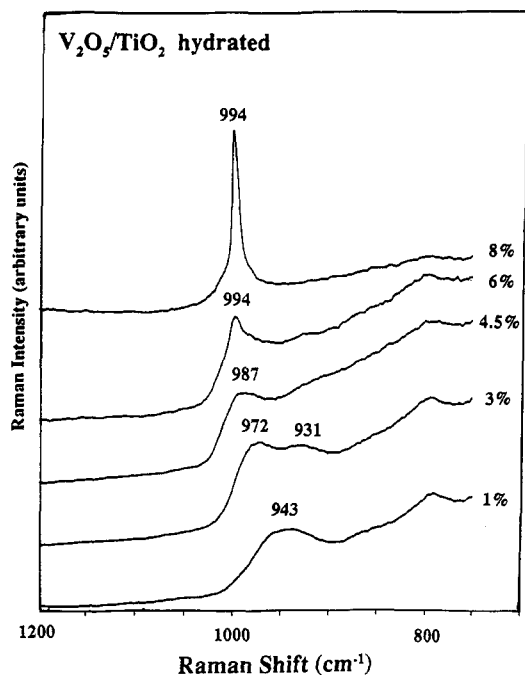
Figure 1. Raman spectra of V_2O_5/TiO_2 under ambient conditions. The vanadium oxide loading increases from 1% to 8%.

Figure 2. Raman spectra of WO_3/TiO_2 under ambient conditions. The tungsten oxide loading increases from 1% to 10%.

have been described elsewhere.[6] The 514.5-nm line of an Argon ion laser (Spectra Physics) was used in both the setups as the excitation source. The laser power at the sample was 40–60 mW for the ambient measurements and 60–100 mW for the in situ measurements.

XPS Surface Analysis. The XPS spectra were obtained on a Model DS800 XPS surface analysis system (Kratos Analytical Plc, Manchester UK). A hemispherical electron energy analyzer was used for electron detection. Mg Kα X-rays at a power of 360 W were employed in this study. Data were collected in 0.75-eV segments for each of the samples. The electron spectrometer was operated in the fixed analyzer transmission (FAT) mode. The samples were prepared by pressing the catalyst powders between stainless steel holders and a polished single-crystal silicon wafer. The powders adhered to the stainless steel holders without requiring additional adhesive materials and possessed relatively flat surfaces. Electrons with take-off angles of 90° from the sample holder plane were selected by the solid angle of acceptance of the focusing lens of the instrument. The XPS measurements were performed at 5×10^{-9} Torr. Elements detected using each spectrum were identified and concentration estimates within the 2–10-nm analyzed layer were made using typical normalization procedures. Sensitivity factors employed in the calculations were selected based on the peak envelope measured for each element of interest. The peaks included in this study were the Ti_{2p} (entire envelope), the W_{4f} (entire envelope), and the $V_{2p3/2}$ (only, to avoid O_{1s} peak interferences). Since the carbon concentrations were relatively low and the kinetic energy positions of the peaks of interest were similar for the elements of interest, the effect of carbon overlayer presence was ignored in this study. This was also unnecessary since only the changes of the surface ration W/Ti [atomic concentrations] against the total tungsten oxide loading and the surface ratio V/Ti [atomic concentrations] against the total vanadium oxide loading were considered in this work.

Results

Raman Spectroscopy. Hydrated: V_2O_5/TiO_2 Hydrated. The Raman spectra for the supported vanadium oxide on TiO_2 samples recorded under ambient conditions are presented in Figure 1. All the spectra show the weak second-order feature of TiO_2 at ~795 cm^{-1}.[25] This TiO_2 band becomes less pronounced as the vanadium oxide coverage is increased because of masking by the colored
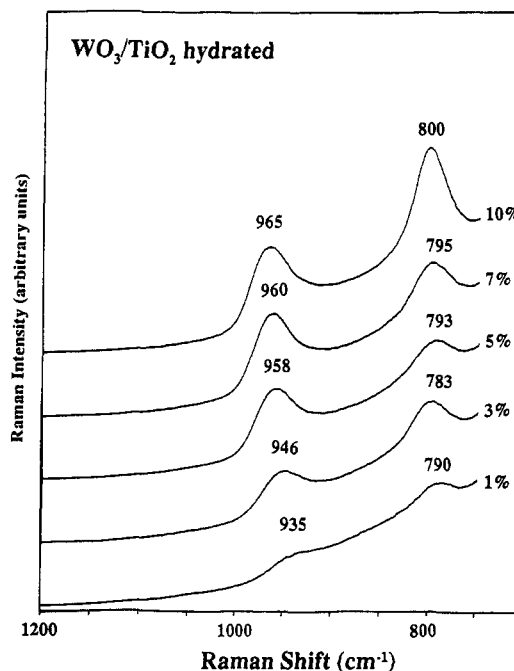
vanadium oxide overlayer. The 1% V_2O_5/TiO_2 sample reveals a broad Raman band at 943 cm^{-1} which shifts upward to 988 cm^{-1} for the 4.5% V_2O_5/TiO_2 sample. These broad bands do not belong to crystalline V_2O_5 and are assigned to the symmetrical V=O stretching modes of two-dimensional surface vanadate species. The Raman spectrum of the 8% V_2O_5/TiO_2 sample shows the sharp and intense band of crystalline V_2O_5 at 994 cm^{-1}. The 6% V_2O_5/TiO_2 sample only possesses a trace of V_2O_5 as indicated by the small 994-cm^{-1} band. Thus, above 6% V_2O_5/TiO_2 the monolayer has been exceeded and crystalline V_2O_5 is present on the titania support. The presence of two-dimensional vanadium oxide species in addition to crystalline V_2O_5 at loadings of 6% and higher cannot be excluded because the strong 994-cm^{-1} band of crystalline V_2O_5 may overshadow other bands.

WO_3/TiO_2 Hydrated. The Raman spectra of WO_3/TiO_2 under ambient conditions are presented in Figure 2. The Raman spectrum of the 1% WO_3/TiO_2 sample shows a weak and broad band at ~935 cm^{-1} which is characteristic of two-dimensional tungsten oxide surface species.[23] In addition to this 935-cm^{-1} band, the second-order feature of TiO_2 at 783 cm^{-1} is also present.[25] As the loading is increased, the W=O stretching mode shifts upward to 965 cm^{-1}. At 10% WO_3/TiO_2, a second intense band at 800 cm^{-1} is observed, showing the presence of crystalline WO_3[26] in addition to the two-dimensional tungsten oxide species (band at 965 cm^{-1}). Thus, a monolayer of tungsten oxide on titania is formed at ~8% WO_3/TiO_2.

V_2O_5–WO_3/TiO_2 Hydrated. Three series of V_2O_5–WO_3/TiO_2 samples have been studied to determine the influence of interaction between vanadium oxide and tungsten oxide on the titania surface. The Raman spectra of the first series, recorded under ambient conditions, are shown in Figure 3. The vanadium oxide loading is 1% and the tungsten oxide loading increases from 0 to 10%. In the absence of tungsten oxide, the Raman spectrum exhibits a weak and broad band at 942 cm^{-1}. This band shifts upwards to 984 cm^{-1} with increasing tungsten oxide loading. The Raman spectrum of the 1% V_2O_5–10% WO_3/TiO_2 sample also reveals the presence of crystalline WO_3 because of the intense band at 800 cm^{-1}.

The Raman spectra of the second set of V_2O_5–WO_3/TiO_2 mixed samples are presented in Figure 4. The vanadium oxide loading is 4.5% and the tungsten oxide loading increases from 0 to 10%. In the absence of tungsten oxide, the Raman spectrum

(25) Beattie, I. R.; Gilson, T. R. *J. Chem. Soc. A* **1969**, 2322.

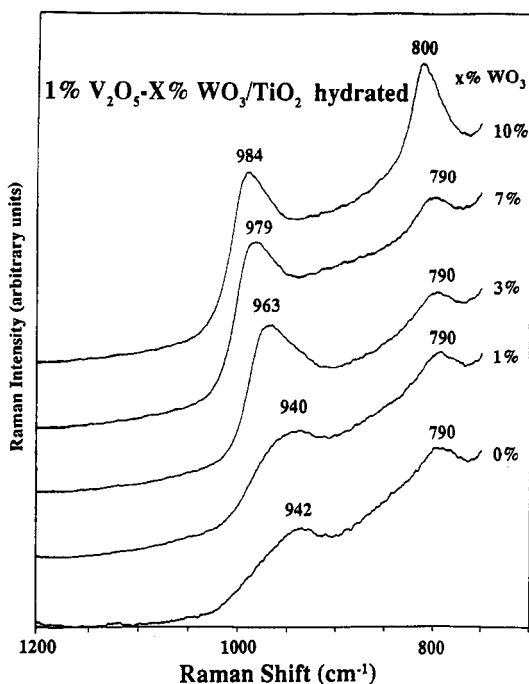(26) Chan, S. S.; Wachs, I. E.; Murrell, L. L. *J. Catal.* **1984**, *90*, 150.

Figure 3. Raman spectra of 1% V$_2$O$_5$–x% WO$_3$/TiO$_2$ under ambient conditions. The tungsten oxide loading, x, increases from 0% to 10%.
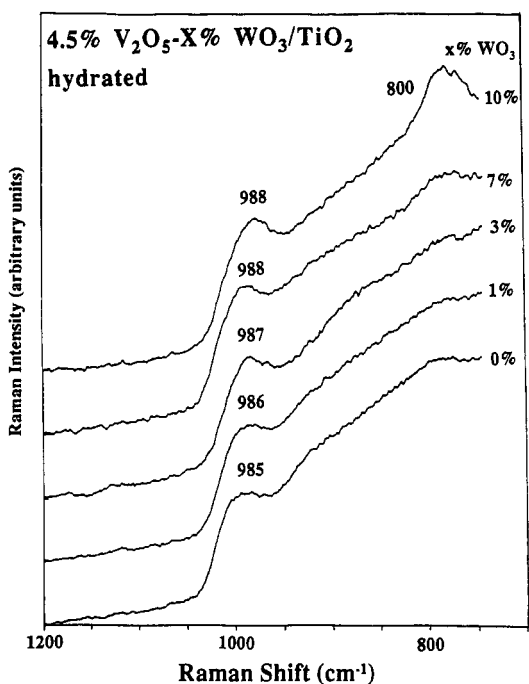

Figure 5. Raman spectra of 6% V$_2$O$_5$–x% WO$_3$/TiO$_2$ under ambient conditions. The tungsten oxide loading, x, increases from 0% to 10%.

Figure 4. Raman spectra of 4.5% V$_2$O$_5$–x% WO$_3$/TiO$_2$ under ambient conditions. The tungsten oxide loading, x, increases from 0% to 10%.

Figure 6. Raman spectra of V$_2$O$_5$/TiO$_2$ under in situ dehydrated conditions. The vanadium oxide loading increases from 1% to 8%.

reveals a broad band at 985 cm^{-1}. Increasing the tungsten oxide loading does not change the position of this band, which shows that the vanadate structure is not influenced by the presence of tungsten oxide species. The 4.5% V$_2$O$_5$–10% WO$_3$/TiO$_2$ sample possesses crystalline WO$_3$ as indicated by the 800-cm^{-1} band. The third set of V$_2$O$_5$–WO$_3$/TiO$_2$ mixed samples contain 6% vanadium oxide and 0–7% tungsten oxide. The 994-cm^{-1} band of crystalline V$_2$O$_5$ becomes a little sharper by the presence of tungsten oxide, but major changes are not observed in Figure 5.

The spectra presented in Figures 3–5 were obtained from titania samples prepared by impregnation with vanadium oxide followed by impregnation with tungsten oxide. The same samples have also been prepared using the inverse sequence of impregnation. The Raman spectra of these samples are identical to those reported above, so the sequence of impregnation does not appear to influence the final molecular structures under ambient conditions.
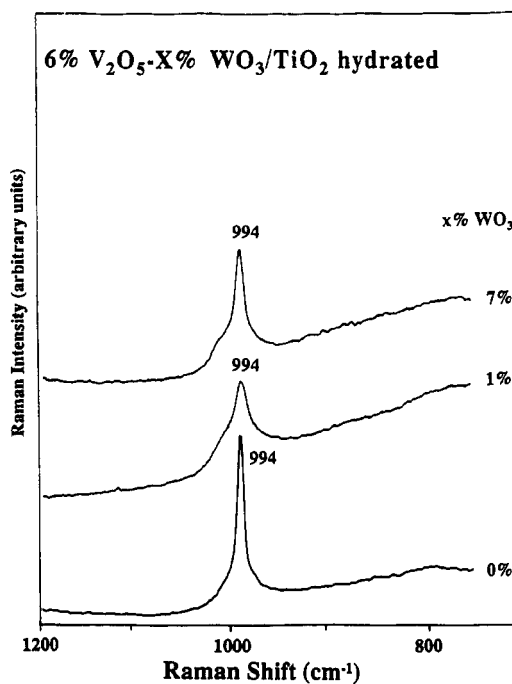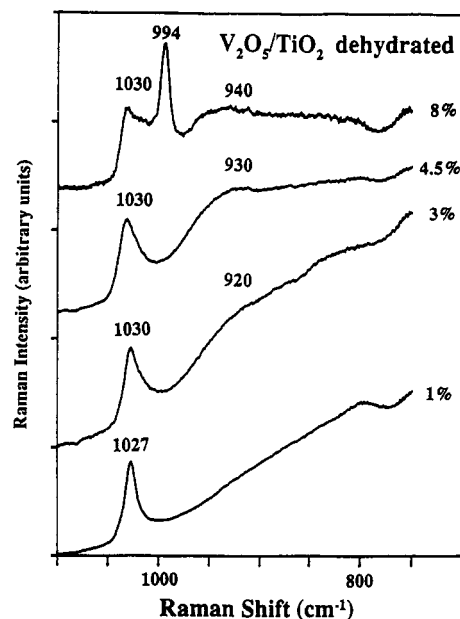
Dehydrated: V$_2$O$_5$/TiO$_2$ Dehydrated. Figure 6 shows the in situ Raman spectra of V$_2$O$_5$/TiO$_2$ recorded at 80 °C after heating at 450 °C in oxygen. All the spectra show a sharp band over 1000 cm^{-1}. This band shifts from 1027 cm^{-1} for the 1% V$_2$O$_5$/TiO$_2$ sample to 1030 cm^{-1} for the higher loading samples. In addition to this sharp band, a second broad band, indicating the presence of a second surface vanadium oxide species, appears at lower wavenumber with increasing vanadium oxide loading. This band shifts from ~920 to ~940 cm^{-1} with increasing vanadium oxide loading. The spectrum of the 8% V$_2$O$_5$/TiO$_2$ sample shows the band of crystalline V$_2$O$_5$ at 994 cm^{-1} in addition to the 1031 and ~940-cm^{-1} bands. This indicates that crystalline V$_2$O$_5$ is not affected by the removal of water molecules and that above monolayer coverage crystalline V$_2$O$_5$ and two-dimensional dehydrated surface vanadium oxide species coexist on the titania surface.

WO$_3$/TiO$_2$ Dehydrated. Upon dehydration, the broad 935-cm^{-1} band of the 1% WO$_3$/TiO$_2$ sample sharpens and shifts to 1010 cm^{-1} as shown in Figure 7. The same results have been obtained
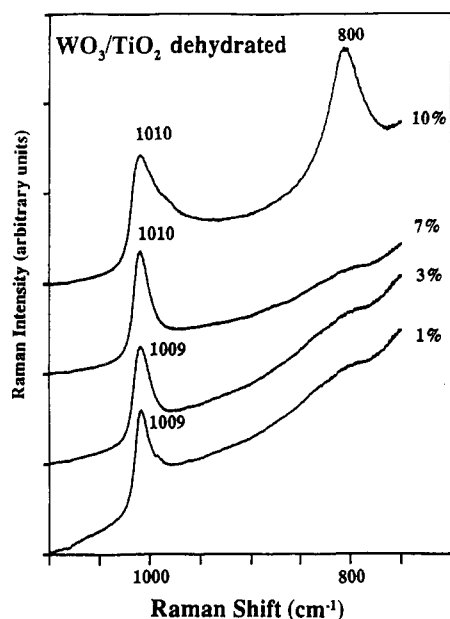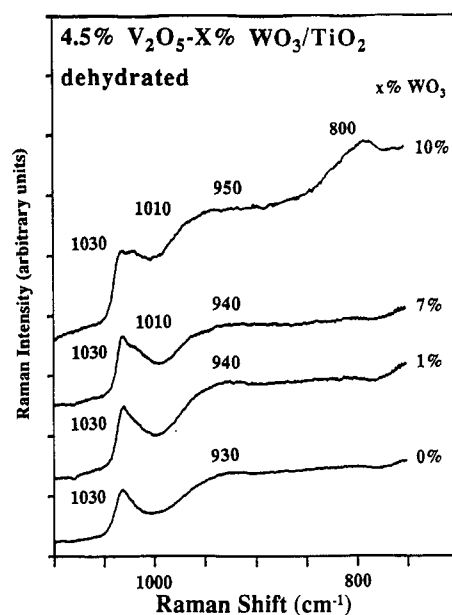
Figure 7. Raman spectra of WO_3/TiO_2 under in situ dehydrated conditions. The tungsten loading increases from 1% to 10%.
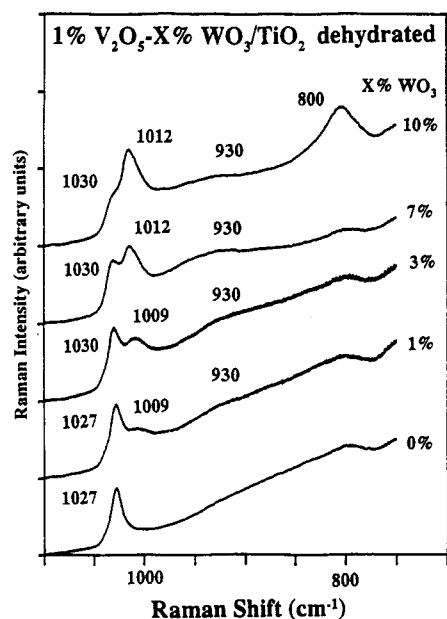
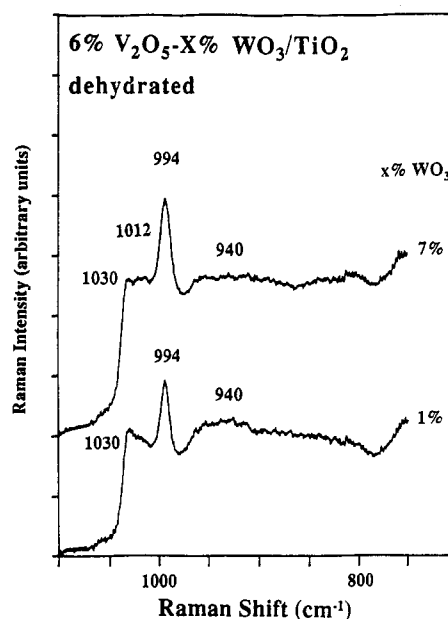**Figure 8.** Raman spectra of 1% V_2O_5-x% WO_3/TiO_2 under in situ dehydrated conditions. The tungsten oxide loading, x, increases from 0% to 10%.

Figure 9. Raman spectra of 4.5% V_2O_5-x% WO_3/TiO_2 under in situ dehydrated conditions. The tungsten oxide loading, x, increases from 0% to 10%.


Figure 10. Raman spectra of 6% V_2O_5-x% WO_3/TiO_2 under in situ dehydrated conditions. The tungsten oxide loading, x, increases from 0% to 7%.

at higher loadings: all the in situ Raman spectra reveal a sharp band at 1010 cm^{-1}. In addition to this band, the Raman spectrum of the 10% WO_3/TiO_2 sample shows the strong 800-cm^{-1} band of crystalline WO_3, which is not affected by the removal of the moisture. Thus dehydration converts the two-dimensional hydrated tungsten oxide species into a surface species which possesses a sharp band at 1010 cm^{-1}. Above monolayer coverage crystalline WO_3 as well as the surface tungsten oxide species exist on the surface as indicated by the presence of both the 1010- and 800-cm^{-1} bands in the Raman spectrum of 10% WO_3/TiO_2.

V_2O_5-WO_3/TiO_2 **Dehydrated.** The in situ Raman spectra of the three sets of V_2O_5-WO_3/TiO_2 mixed samples are presented in Figures 8-10. The Raman spectrum of the 1% V_2O_5-1% WO_3/TiO_2 sample (Figure 8) shows a sharp band at 1027 cm^{-1}, which is similar to the 1% V_2O_5/TiO_2 sample. In addition to this 1027-cm^{-1} band, a shoulder is observed at 1010 cm^{-1}, the intensity of which increases with increasing tungsten oxide loadings. This 1010-cm^{-1} band is identical to the band observed for the in situ Raman spectra of WO_3/TiO_2. The spectrum of the 1% V_2O_5-1% WO_3/TiO_2 sample shows that the cross-section of dehydrated

surface vanadium oxide species is ~4 times larger than the cross-section of the dehydrated tungsten oxide species. As the loading is increased to 10% tungsten oxide, crystalline WO_3 is observed on the titania surface by the presence of the 800-cm^{-1} band. Also a weak band at ~930 cm^{-1} shows up with increasing tungsten oxide loadings.

The Raman spectra of the second set of 4.5% V_2O_5-(0-10)% WO_3/TiO_2 mixed samples basically reveal the same trend as the Raman spectra of the 1% V_2O_5-(0-10)% WO_3/TiO_2 samples: two bands are present at 1030 and 1010 cm^{-1} with an intensity ratio that changes with increasing tungsten oxide loadings. All the spectra show also a broad band at ~930 cm^{-1} which shifts to ~950 cm^{-1} with increasing tungsten oxide loading. It is difficult to determine if the intensity of this broad band also increases with increasing tungsten oxide loading. The 4.5% V_2O_5-10% WO_3/TiO_2 sample possesses crystalline WO_3 on its surface since the 880-cm^{-1} band is present.

The Raman spectra of 6% V_2O_5-(0-7)% WO_3/TiO_2 are shown in Figure 10. In addition to the 994-cm^{-1} band of crystalline V_2O_5,
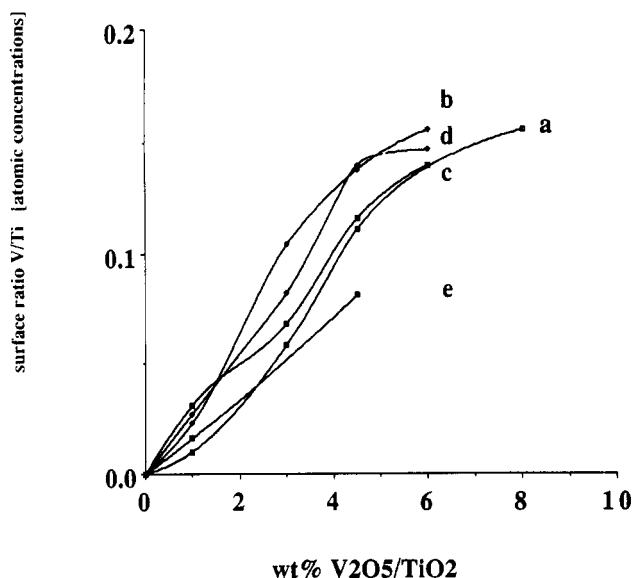
Figure 11. XPS surface ratio V/Ti versus total % V$_2$O$_5$: (a) V$_2$O$_5$/TiO$_2$; (b) V$_2$O$_5$-1% WO$_3$/TiO$_2$; (c) V$_2$O$_5$-3% WO$_3$/TiO$_2$; (d) V$_2$O$_5$-7% WO$_3$/TiO$_2$; (e) V$_2$O$_5$-10% WO$_3$/TiO$_2$.

Figure 12. XPS surface ratio W/Ti versus %WO$_3$: (a) 0% V$_2$O$_5$-WO$_3$/TiO$_2$; (b) 1% V$_2$O$_5$-WO$_3$/TiO$_2$; (c) 4.5% V$_2$O$_5$-WO$_3$/TiO$_2$; (d) 6% V$_2$O$_5$-WO$_3$/TiO$_2$.

a bands at 1030 cm^{-1} is observed for the 6% V$_2$O$_5$-1% WO$_3$/TiO$_2$ and two bands at 1030 and $\sim$1012 cm^{-1} are observed for the 6% V$_2$O$_5$-7% WO$_3$/TiO$_2$ sample. This indicates that under dehydrated conditions crystalline V$_2$O$_5$ is not influenced by the tungsten oxide species and that above monolayer loading crystalline V$_2$O$_5$ as well as two-dimensional vanadium oxide and tungsten oxide species exist on the titania surface. The influence of 1% WO$_3$ is less visible because of the low Raman cross-section of the dehydrated tungsten oxide species.

XPS Surface Studies. Vanadium Oxide. The surface V/Ti ratios [atomic concentrations], determined from the XPS measurements, versus the total vanadium oxide loading of the V$_2$O$_5$-(0–10)% WO$_3$/TiO$_2$ samples are presented in Figure 11. For the V$_2$O$_5$/TiO$_2$ samples the V/Ti surface ratio increases almost linearly with the total vanadium oxide content until $\sim$4.5%. For higher loadings the surface ratio V/Ti increases slowly with the total V$_2$O$_5$ loading as indicated by the small slope of the curve above 4.5%. These results are in agreement with our Raman data and previous reported XPS measurements.[27,28] The change in slope has been explained by the fact that XPS can detect most of the surface metal oxide atoms up to monolayer coverage (so the XPS signal is directly proportional with the vanadium oxide surface content). Above monolayer loading the XPS signal increases very slowly because only those electrons which are emitted through the monolayer or from the top of the crystals are detected.[27] This dependence has been previously used to study the dispersion of a metal oxide on a high surface area surface. If the metal oxide is poorly dispersed, the change in slope occurs at lower total metal oxide loading and vice versa.[27–30]

Increasing the tungsten oxide loading from 0% (Figure 11a) to 10% (Figure 11e) does not significantly change the shape of the curve or the position at which the slope of the curve decreases. This indicates that the dispersion of the vanadium oxide is not influenced by the presence of tungsten oxide species on the titania surface.

Tungsten Oxide. Figure 12a reveals the dependence of the W/Ti surface ratio [atomic concentrations] on the total tungsten oxide loading for the WO$_3$/TiO$_2$ samples. The surface ratio W/Ti increases linearly with the total tungsten oxide loading up to $\sim$7%. Raman spectroscopy demonstrated that at higher loadings, crystalline WO$_3$ is present on the surface and the surface ratio
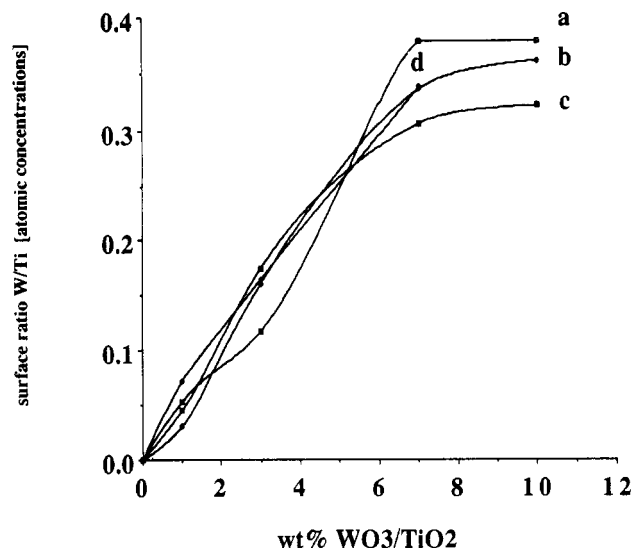
W/Ti does not increase, as demonstrated by the plateau observed in Figure 12a. In the presence of vanadium oxide the surface W/Ti ratios versus the total WO$_3$ curves do not change (Figure 12, parts b–e). This shows that the presence of vanadium oxide does not influence the dispersion of the tungsten oxide phase on the TiO$_2$.

Discussion

Hydrated: V$_2$O$_5$/TiO$_2$ **Hydrated.** In aqueous solution the molecular structure of vanadium oxide is a function of pH and vanadium oxide concentration.[31] Decreasing the solution pH or increasing the vanadium oxide concentration results in a structural change from tetrahedral to more complex octahedrally coordinated structures. In a recent publication Deo and Wachs[16] showed that under ambient conditions the structural dependence with loading for supported vanadium oxide is similar to what is observed in aqueous solution. Under supported conditions the vanadium oxide molecular structures were found to be a function of the net pH at the point of zero surface charge (pzc) which depends on the type of support and the vanadium oxide surface coverage. The pzc value of TiO$_2$ has been determined to be 5–6.[32] Increasing the vanadium oxide loading decreases the net pH at pzc because of the acidic nature of vanadium oxide (pzc of 1.5).

The shift from 943 cm^{-1} for the 1% V$_2$O$_5$/TiO$_2$ sample to 987 cm^{-1} for the 4.5% V$_2$O$_5$/TiO$_2$ sample is in agreement with previously reported Raman spectra[6–9,12,16] and suggests that under ambient conditions different two-dimensional vanadium oxide species may be present in the V$_2$O$_5$/TiO$_2$ samples. Based upon these band positions alone, however, it is impossible to determine the nature of these species since tetrahedral and octahedral, monomeric and polymeric vanadium oxide species give rise to bands in the 1200–800-cm^{-1} region.[33] Additional vanadia modes, which are critical for a complete structural analysis, are obscured by titania, which itself exhibits very strong Raman bands below 700 cm^{-1}.[25] Recently the Raman spectra of V$_2$O$_5$/γ-Al$_2$O$_3$ have been reported under ambient conditions.[9,30,34,35] Since γ-Al$_2$O$_3$ is Raman inactive, vanadium oxide Raman bands could be detected down to $\sim$100 cm^{-1}. At low loadings, the Raman spectrum of V$_2$O$_5$/γ-Al$_2$O$_3$ revealed bands at 940 cm^{-1} and weak bands at

(27) Bond, G. C.; Zurita, J. P.; Flamerz, S. *Appl. Catal.* **1986**, *27*, 353.

(28) Liu, Z.; Lin, Z.; Kan, H.; Li, F. *Appl. Phys. A* **1988**, *45*, 159.

(29) Taouk, B.; Guelton, M.; Grimblot, J.; Bonell, J. P. *J. Phys. Chem.* **1988**, *92*, 6700.

(30) Le Coustumer, L. R.; Taouk, B.; Le Meur, M.; Payen, E.; Guelton, M.; Grimblot, J. *J. Phys. Chem.* **1988**, *92*, 1230.

(31) Baes, C. F., Jr.; Mesmer, R. E. *The Hydrolysis of Cations*; Wiley and Sons Inc.: New York, 1986.

(32) Anderson, J. R. *Structure of Metallic Catalysts*; Academic Press: New York, 1975.

(33) Griffith, W. P.; Lesniak, P. J. B. *J. Chem. Soc. A* **1969**, 1066.

(34) Deo, G.; Hardcastle, F. D.; Richards, M.; Wachs, I. E. *ACS Petrol. Chem. Div. Preprints* **1989**, *34*(3), 529.

(35) Deo, G.; Hardcastle, F. D.; Richards, M.; Wachs, I. E.; Hirt, A. *New Catalytic Materials*; Baker, R. T., Murrell, L. L., Eds.; ACS Symp. Series; American Chemical Society: Washington, DC, 1990.

~550 and 220 cm^{-1}. These bands corresponded to those found in tetrahedrally coordinated polymeric vanadates and were therefore assigned to surface metavanadate species. At moderate loadings a new band was observed at ~990 cm^{-1} which was accompanied by several weak bands at lower frequencies. These bands matched best the Raman bands of the decavanadate cluster, $V_{10}O_{28}^{6-}$, which has a distorted octahedral structure.[36] Comparison of the Raman spectra of V_2O_5/TiO_2 with the Raman spectra of V_2O_5/γ-Al_2O_3 demonstrates that the 940-cm^{-1} band in the 1% V_2O_5/TiO_2 spectrum is associated with tetrahedrally coordinated metavanadate and the 988-cm^{-1} band at 4.5% V_2O_5/TiO_2 arises from to octahedrally coordinated vanadium oxide species, which best match the decavanadate cluster.

Additional information to support this assignment has recently been obtained by solid-state ^{51}V NMR and FTIR. Solid-state ^{51}V NMR showed that at low loading vanadium oxide favors a tetrahedral coordination on titania while at higher loadings almost all the vanadium oxide is directed into octahedral sites.[19] A recent FTIR study of a hydrated 10% V_2O_5/TiO_2 sample showed, in addition to the IR band of crystalline V_2O_5 at 1015 cm^{-1}, a broad band at 990 cm^{-1} and a weak band at 940 cm^{-1}.[11] The 990-cm^{-1} band matches the IR stretching mode of the decavanadate cluster which is found in the 950–1000-cm^{-1} region.[37] Thus, the combination of ^{51}V NMR, FTIR, and Raman spectroscopy reveals that under hydrated conditions two vanadium oxide species are present in the V_2O_5/TiO_2 samples: a metavanadate species, which possesses distorted tetrahedral symmetry, and a decavanadate species which has a distorted octahedral coordination. Their relative concentrations vary with the vanadium oxide coverage. At 6% V_2O_5/TiO_2 monolayer coverage has been exceeded, and crystalline V_2O_5 is also present on the titania surface. This is in agreement with the XPS data which show that the V/Ti surface ratio increased only slowly with the total vanadium oxide content above 4.5% V_2O_5/TiO_2.

WO$_3$/TiO$_2$ Hydrated. The molecular structure of the supported tungsten oxide species also follows the trend predicted by the net pH of zero surface charge which is a function of the surface pH of the support and the tungsten oxide loading.[16] The Raman spectra of the WO$_3$/TiO$_2$ samples under ambient conditions suggest that below 8% different two-dimensional tungsten oxide species are present, indicated by the shift from ~935 cm^{-1} for the 1% WO$_3$/TiO$_2$ sample to 960 cm^{-1} for the 8% WO$_3$/TiO$_2$ sample. Above 8% WO$_3$/TiO$_2$, monolayer coverage has been exceeded and WO$_3$ crystals are also present on the TiO$_2$ surface. This is supported by the XPS data which show that above 8% WO$_3$/TiO$_2$ the surface W/Ti ratio does not increase with increasing tungsten oxide loading (indicating the presence of a crystalline phase). The identification of the different two-dimensional tungsten oxide species is somewhat hampered by the strong TiO$_2$ Raman features below 700 cm^{-1}, which prevent the detection of additional tungsten oxide bands. The 935-cm^{-1} band, observed in the Raman spectrum of the 1% WO$_3$/TiO$_2$ samples, matches the symmetrical stretching mode of tetrahedrally coordinated tungsten oxide in aqueous solution, WO_4^{2-} (symmetrical stretching mode at 931 cm^{-1}[33]). This assignment is in agreement with the WO$_3$/γ-Al_2O_3 system where combined Raman and XANES data revealed the presence of distorted tetrahedral coordination at low loading.[38] The 960-cm^{-1} band in the Raman spectrum of the 8% WO$_3$/TiO$_2$ sample is assigned to the stretching mode of solvated polytungstate species such as $W_6O_{10}(OH)^{5-}$(aq), $W_{12}O_{39}^{6-}$(aq), or $W_{12}O_{41}^{10-}$(aq), which all have a distorted octahedral coordination.[31] This assignment is based upon the similarity of the Raman spectrum of WO$_3$/γ-Al_2O_3 system at higher loadings, which exhibits a band at ~980 cm^{-1} accompanied by bands at 330, 215, and 550 cm^{-1}. The latter two band are diagnostic of W–O–W linkages found in solvated polytungstate clusters.[33] The presence of tetrahedrally coordinated tungsten

oxide species at low loading and octahedrally coordinated tungsten oxide species at moderate loadings under ambient conditions is similar to the structural dependence of tungsten oxide in aqueous solutions.[31]

V$_2$O$_5$–WO$_3$/TiO$_2$ Hydrated. The above Raman assignments for the single V_2O_5/TiO_2 and WO$_3$/TiO$_2$ systems are now used to interpret the Raman bands of the V_2O_5–WO$_3$/TiO$_2$ mixed samples. The first set of mixed samples contain 1% V_2O_5 and (0–10)% WO$_3$/TiO$_2$ and was chosen to study the influence of tungsten oxide on the molecular structure of metavanadate species. At first sight it is not clear if the broad band in the 942–984-cm^{-1} region in Figure 3 belongs to vanadium oxide species, tungsten oxide species, or to both. However, the broad band shifts to 988 cm^{-1} while no tungsten oxide species has been observed on titania which exhibits a stretching band over 965 cm^{-1} as shown in Figure 2. Furthermore, as shown above, the Raman cross-section of the dehydrated vanadium oxide species is ~4 times bigger than the Raman cross-section of the dehydrated tungsten oxide species. If one assumes that the cross-sections of the hydrated species are similar to those of the dehydrated species, then it is likely that the Raman bands of hydrated tungsten oxide species are overshadowed by the stronger vanadium oxide stretching mode. The 984-cm^{-1} band matches the Raman band of the decavanadate cluster, as shown above. Thus, the Raman spectra reveal that the hydrated metavanadate species are replaced by hydrated decavanadate species with increasing tungsten oxide loading. This effect occurs because under ambient conditions the vanadium oxide structure is dependent on the net surface pH at pzc.[16] Increasing the tungsten oxide loading increases the aqueous acidity and the net pH at pzc decreases resulting in conversion of the metavanadate species to decavanadate species.

The second set contains 4.5% V_2O_5 and (0–10)% WO$_3$ and was chosen to determine the influence of the presence of tungsten oxide on the decavanadate structure and because 4.5% V_2O_5 on titania is slightly below monolayer coverage in the single V_2O_5/TiO_2 system. In the absence of tungsten oxide, the Raman spectrum reveals the presence of decavanadate species by the 985-cm^{-1} band. Increasing the tungsten oxide loading does not change the position of this band, which shows that the decavanadate structure is not affected by the presence of tungsten oxide under ambient conditions. In the absence of tungsten oxide, the net pH at pzc is low since decavanadate species are present. Adding tungsten oxide does not influence the decavanadate species because an acidic aqueous solution is being added to an acidic system, and only the decavanadate structure is stable in acidic aqueous solutions.[31]

The third set of samples contain 7% V_2O_5 and (0–7)% WO$_3$. Crystalline V_2O_5 is observed for all the samples. The 994-cm^{-1} band becomes slightly more intense by the presence of tungsten oxide which may indicate that the dispersion of the vanadium oxide is decreased by the tungsten oxide species. This, however, is not supported by the XPS data which suggest that the spreading of vanadium oxide on the titania surface is not affected by the presence of tungsten oxide.

The Raman spectra, presented for the hydrated V_2O_5–WO$_3$/TiO$_2$ samples, yield little information about the influence of the presence of vanadium oxide on the two-dimensional structure of the tungsten oxide species. This is because the Raman bands of the surface tungsten oxide species are overshadowed by the stronger Raman bands of the surface vanadium oxide species. However, the two-dimensional tungsten oxide species are expected to follow the same trend as the vanadium oxide species since the net pH at pzc dependence is generally applicable.[16] Thus, the tetrahedrally coordinated tungsten oxide species are expected to change into octahedrally coordinated tungsten oxide species with increasing vanadia content due to the acidic nature of vanadium oxide. All the mixed oxide samples containing 8% WO$_3$ show the presence of crystalline WO$_3$ by the 800-cm^{-1} band. The 800-cm^{-1} band, however, is less intense in the presence of vanadium oxide. This can be explained by the fact that the single WO$_3$/TiO$_2$ samples are white which would make them very good Raman scatterers, while mixed samples are dark yellow due to the vanadium(V) oxide and, therefore poorer Raman scatterers. Thus,

(36) Evans, H. T. *Inorg. Chem.* **1966**, *5*, 967.
(37) Frederickson, L. D., Jr.; Hansen, D. M. *Anal. Chem.* **1963**, *35*, 818.
(38) Horsley, J. A.; Wachs, I. E.; Brown, J. M.; Via, G. H.; Hardcastle, F. D. *J. Phys. Chem.* **1987**, *91*, 4014.
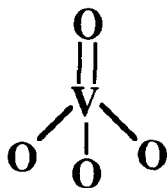
Figure 13. Schematic representation of the highly distorted surface vanadium oxide species.

Figure 14. Schematic representation of the octahedrally coordinated surface tungsten oxide species.

crystalline WO_3 is not influenced by the presence of vanadium oxide species. This is supported by the XPS measurements which show that in the presence or absence of vanadium oxide monolayer coverage of tungsten oxide is reached at ~7% WO_3. Raman spectroscopy demonstrates that under ambient conditions only the metavanadate structure is influenced by the presence of tungsten oxide. A similar effect has recently been reported for V_2O_5/TiO_2 and V_2O_5/γ-Al_2O_3 catalysts[19b,34,35] contaminated with alkaline impurities [Na, K].

Dehydrated: V₂O₅/TiO₂ Dehydrated. The in situ Raman spectra reveal that below monolayer coverage (<6% V_2O_5/TiO_2) two different vanadium oxide species are present on the dehydrated titania surface. One species is highly distorted and exhibits a sharp Raman band at 1030 cm⁻¹. This species is present at all loadings. Recent ^{51}V NMR measurements have revealed that the highly distorted vanadium oxide species has distorted tetrahedral coordination and that the tetrahedron possesses cylindrical symmetry.[19] The species only exhibits one Raman band at 1030 cm⁻¹ which indicates that this species is monooxo (one short V=O bond) since a dioxo (two V=O bonds) species would show two V=O stretching modes if the two V=O bonds were inequivalent and three bands if the two V=O bonds were equivalent (symmetrical stretch, asymmetrical stretch, and bending mode). Cristiani et al.[11] reported an IR band at 1035 cm⁻¹ for a 10% V_2O_5/TiO_2 sample under dehydrated conditions. The coincidence of the Raman band at 1030 cm⁻¹ and the IR band at 1035 cm⁻¹ supports the monooxo model since a dioxo vanadate species would exhibit a more intense asymmetric stretching mode of the O—V—O group, while the Raman band would show a more intense symmetrical stretching mode. Thus, the combined ^{51}V NMR, FTIR, and Raman data show that the highly distorted vanadium oxide species has a distorted tetrahedral structure with one short V=O bond (monooxo).

However, based upon these data alone it is not possible to present a more precise structure. Progress has been made in determining the molecular structure of V_2O_5/γ-Al_2O_3 by applying the diatomic approximation method, presented by Hardcastle et al.[39] They established an empirical stretching frequency/bond distances correlation by considering each V–O bond as a totally independent oscillator. The Raman spectrum of the V_2O_5/γ-Al_2O_3 sample shows two Raman bands under dehydrated conditions, similar to the V_2O_5/TiO_2 system at 1026 cm⁻¹ (sharp) and 850 cm⁻¹ (broad). On the basis of the diatomic approximation method, Hardcastle et al. were able to determine the V–O bond distances of the highly distorted vanadate species and to propose a more precise structure. Since the Raman, FTIR, and ^{51}V NMR data are similar for the V_2O_5/TiO_2 and V_2O_5/γ-Al_2O_3 systems,[19,39] and the same structure is proposed for the V_2O_5/TiO_2 system.

The second dehydrated vanadate species is moderately distorted and has a broad Raman band at ~920 cm⁻¹ which shifts to ~940 cm⁻¹ with increasing loading. The second species becomes more pronounced at higher loadings. This second vanadate species should also possess a tetrahedrally coordinated structure because in situ ^{51}V NMR showed only the presence of tetrahedrons.[19] Hardcastle et al. suggested that for the V_2O_5/γ-Al_2O_3 system, two different, moderately distorted, tetrahedrally coordinated structures are possible.[39] The first one is a monooxo structure,
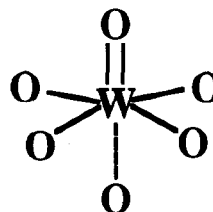
similar to the highly distorted structure but with different V=O and V—O bond distances. The V—O bonds were found to be consistent with possible V—OH bonds. The second possible structure is a dioxo which possesses two terminal V=O bonds and two bridging V—O bonds. It was argued that the V—O bonds were consistent with possible V—O—V linkages. Thus, the moderately distorted monooxo vanadate species is hydroxylated and isolated, whereas the dioxo is polymeric. A polymeric structure has also been proposed by other authors.[10,11]

WO₃/TiO₂ Dehydrated. Upon dehydration, the broad bands in the 935–960-cm⁻¹ region disappear and are replaced by a single band at 1010 cm⁻¹ for all the tungsten oxide loadings. This shows that the dehydration drastically changes the molecular structures and that the two-dimensional tetrahedrally coordinated WO_4^{2-} as well as the distorted octahedrally coordinated polytungstate species are converted into the same surface tungsten oxide species. This is in contrast with in situ Raman data of the WO_3/γ-Al_2O_3 system which show two bands, a sharp band at 1016 cm⁻¹ and a weak, broad band at ~870 cm⁻¹,[6,39,40,41] which indicates the presence of two different surface tungsten oxide species. The corresponding molecular structures in WO_3/γ-Al_2O_3 have recently been determined by Hardcastle et al.[39] The 1016-cm⁻¹ Raman band matches the IR absorption at 1015 cm⁻¹. This indicated that the highly distorted tungsten oxide has a monooxo structure. Based upon the diatomic approximation method, a highly distorted octahedrally coordinated structure was proposed with one short W=O bond, one long opposing W—O bond and four bridging W—O bonds. The WO_3/TiO_2 system shows a similar 1010-cm⁻¹ Raman band and recent in situ XANES provided evidence for a highly distorted octahedrally coordination of the tungsten oxide on the TiO₂ surface.[42] Therefore the same highly distorted octahedrally coordinated structure is proposed for the WO_3/TiO_2 system (Figure 14).

The second broad band at ~870-cm⁻¹ in the spectra of the WO_3/γ-Al_2O_3 system has not been observed in the Raman spectra of the WO_3/TiO_2 system. The inability to detect this weak, broad band may be caused by the increasing slope in the Raman spectrum due to the strong 639-cm⁻¹ band as well as the weaker 790-cm⁻¹ band of TiO₂. If, however, the second surface species is not present on the titania surface, then a possible explanation is that the formation of two types of surface tungsten oxide species on alumina is associated with the presence of specific surface hydroxyl groups. It is known that alumina possesses different surface hydroxyl groups than titania[43] which may explain the presence of two types of surface tungsten oxide species on the alumina surface and one type of surface tungsten oxide species on the titania surface.

V₂O₅-WO₃/TiO₂ Dehydrated. Under ambient conditions it has been demonstrated that the two-dimensional metal oxide species are surrounded by water molecules and, therefore, more or less shielded from the support surface. Heating the catalyst removes the water and, consequently, increases the interaction with the support. For supported metal oxide systems where more than one

(39) (a) Hardcastle, F. D. Dissertation, Lehigh University. University Microfilms International: Ann Arbor, MI, p 1190. (b) Hardcastle, F. D.; Wachs, I. E. submitted to *J. Phys. Chem.* (c) Hardcastle, F. D.; Turek, A. M.; Jenhg, J. M.; Vuurman, M. A.; Deo, G.; Wachs, I. E., to be published.

(40) Payen, E.; Kasztelan, S.; Grimblot, J.; Bonelle, J. P. *J. Raman Spectrosc.* **1984**, *15*, 282.

(41) Stencel, J. M.; Makovsky, L. E.; Diehl, J. R.; Sarkus, T. A. *J. Raman Spectrosc.* **1984**, *15*, 282.

(42) Wachs, I. E., unpublished results.

(43) Boehm, H.-P.; Knözinger, H. *Catalysis, Science and Technology*; Anderson, J. R., Boudart, M., Eds.; Springer-Verlag: Berlin, 1983; Vol. 4, p 39.

type of metal oxide is present a number of scenarios could occur upon dehydration: (a) The different types of surface metal oxides interact strongly and new hetero surface metal oxide species are formed. (b) The different types of surface metal oxides exist independently from each other on the support. (c) One of the surface metal oxide species interacts more strongly with the support than the second surface metal oxide species. The dispersion of the latter metal oxide is consequently decreased and the metal oxide is forced to change its two-dimensional structure, to form a three-dimensional crystalline phase or sit on top of the former metal oxide overlayer. (d) One of the surface metal oxide species is adsorbed *on* the support surface, and the second metal oxide species is absorbed *into* the support surface.

These various possibilities will be investigated below. The in situ Raman spectra of the mixed V_2O_5–WO_3/TiO_2 samples reveal that dehydration drastically changes the molecular structures of the surface species. This demonstrates that both the vanadium oxide and the tungsten oxide are present *on* the support and not *in* the support since metal oxides which are located *in* the support are not influenced by the presence of water molecules.[23]

A vanadium oxide loading of 4.5% V_2O_5 is slightly below monolayer coverage in the single V_2O_5/TiO_2 system and an 8% tungsten oxide loading is approximately below monolayer coverage in the single WO_3/TiO_2 system. Therefore, it is expected that the greatest interaction between both metal oxides with regard to their two-dimensional structures would occur in the 4.5% V_2O_5–8% WO_3/TiO_2 sample. The in situ Raman spectrum of this sample, however, only shows the 1030-cm^{-1} band of the highly distorted vanadium oxide species, the 930–950-cm^{-1} band of moderately distorted vanadium oxide species and the 1010-cm^{-1} band of the octahedrally coordinated tungsten oxide species. The band positions of two-dimensional metal oxides are sensitive to the support type under dehydrated conditions. The in situ Raman band of the highly distorted vanadium oxide species in V_2O_5/TiO_2 is found at 1030 cm^{-1} while e.g. 1042 cm^{-1} has been reported for V_2O_5/SiO_2.[10] For WO_3/TiO_2, the Raman band position of the distorted octahedral is 1010 cm^{-1}, while e.g. 1016 cm^{-1} has been found for WO_3/γ-Al_2O_3.[39] Although the 1030- and 1010-cm^{-1} bands in the Raman spectrum of the mixed 4.5% V_2O_5–8% WO_3/TiO_2 are not well resolved, the spectrum shows that these band positions are basically the same as the positions observed in the single component V_2O_5/TiO_2 and WO_3/TiO_2 systems, respectively. It can, therefore, be concluded that the highly distorted vanadium oxide and the octahedrally distorted tungsten oxide species are present *on* the TiO_2 support and not one on top of the other. Raman spectroscopy is a sensitive technique for the detection of metal oxide crystals, but the formation of crystalline V_2O_5 or crystalline WO_3 was not observed in the 4.5% V_2O_5–8% WO_3/TiO_2 sample. This is in agreement with the XPS data which also show that the dispersion of both metal oxides is not influenced by the presence of the other metal oxide.

Sutsuma et al. investigated the molecular structure of the bulk and the surface of V_2O_5–WO_3 catalysts. It was concluded that although V_2O_5 and WO_3 are not well mixed in the bulk of the catalyst, V and W ions are well-mixed in the surface of the catalyst.[3] We have not observed any new Raman features which would indicate the formation of V–O–W species. However, it is possible that very small amounts of V–O–W species are present on the surface. Thus, the Raman spectra show that the highly distorted surface vanadium oxide species and the highly distorted octahedrally coordinated surface tungsten oxide species essentially exist independently of each other on the titani surface. This is consistent with scenario b. However, there is an indication that the moderately distorted surface vanadium oxide is influenced by the presence of surface tungsten oxide. The 1% V_2O_5–(1–10)% WO_3/TiO_2 samples shows a Raman band at ~930 cm^{-1} and this band shifts from ~930 to ~950 cm^{-1} in the spectra of 4.5% V_2O_5–(1–10)% WO_3/TiO_2 with increasing tungsten oxide loading. In the absence of tungsten oxide, the moderately distorted vanadium oxide species is not observed in the 1% V_2O_5/TiO_2, but is formed at higher vanadium oxide loadings where the band position shifts upwards with increasing vanadium loading. So,

in the presence of tungsten oxide, the moderately distorted surface vanadium oxide species becomes more abundant. This is in agreement with scenario c according to which one surface metal oxide is forced to change into a different two-dimensional structure due to the presence of the second surface metal oxide species. Thus for the mixed V_2O_5–WO_3/TiO_2 samples scenario b seems to operate at low coverage while at higher coverage both scenarios b and c are operational.

A simple two-dimensional monolayer model does not explain how the titania surface can simultaneously accommodate a monolayer of vanadium oxide species and a monolayer of tungsten oxide species. A possible explanation is that the different surface species are interacting with different surface hydroxyl groups. The highly distorted surface vanadium oxide species and the surface tungsten oxide species may be interacting with two different types of surface OH groups and, therefore, do not "feel" each other. An FTIR study on the different hydroxyl groups could help clarify this matter.

Although the DeNO$_x$ reaction has been the subject of numerous investigations, the nature of the active species and reaction mechanism is still undetermined. It is generally agreed that the first step involves the adsorption of NH_3 on the catalyst surface. Inomata et al.[44] proposed that NH_3 is adsorbed as NH_4^+, interacting with both a surface V=O group and a surface V—OH group. Wong et al.[45] slightly modified this model while Janssen et al.[46] proposed that NH_3 is chemisorbed on two surface V=O groups producing V—ONH_2 and V—OH. Busca[47] argued that the first step involves the breaking of the N–H bond of molecular coordinated ammonia on surface VO^{2+} cations. Gasior et al.[48] proposed that only V—OH act as the active site which has recently been supported by Chen et al. who performed an extended Hückel molecular orbital calculation on a model V_2O_5/TiO_2 surface.[49] It has further been shown that the activity of the DeNO$_x$ reaction over V_2O_5/TiO_2 increases with increasing vanadia content up to ~7% V_2O_5.[44b] An IR study revealed that V_2O_5/TiO_2 possesses Brønsted acid sites which were associated with the surface vanadia species since titania does not possesses Brønsted acidity.[50] The Brønsted acidity follows the same trend as the activity for the DeNO$_x$ reaction and increases with increasing vanadia loading up to ~5% V_2O_5. Okazaki et al.[51] also demonstrated that Brønsted acidity is required for the DeNO$_x$ reaction. Our study shows that under dehydrated conditions the moderately distorted vanadium oxide species become more abundant with increasing vanadia coverage. Hardcastle et al.[38] argued that the moderately distorted vanadium oxide species possibly possesses OH groups. It is therefore suggested that the moderately distorted vanadium oxide species is possibly the precursor of the active site in the DeNO$_x$ reaction. The role of the tungsten oxide species, which seem to enhance the formation of the moderately distorted vanadium oxide species, is yet not totally clear. On alumina, other metal oxide such as molybdenum oxide, tungsten oxide, iron oxide, cobalt oxide, and nickel oxide also seem to enhance the formation of the moderately distorted vanadium.[52]

Conclusions

The molecular structures of V_2O_5/TiO_2, WO_3/TiO_2, and V_2O_5–WO_3/TiO_2 catalytic systems have been studied by Raman spectroscopy under hydrated and dehydrated conditions and by

(44) (a) Inomata, M.; Miyamoto, A.; Murakami, Y. *J. Catal.* **1980**, *62*, 140. (b) Inomata, M.; Miyamoto, A.; Ui, T.; Kobayashi, K.; Murakami, Y. *Ind. Eng. Chem. Prod. Res. Dev.* **1982**, *21*, 424. (c) Miyamoto, A.; Kobayashi, K.; Inomata, M.; Murakami, Y. *J. Phys. Chem.* **1982**, *86*, 2945.

(45) Wong, W.; Nobe, K. *Ind. Eng. Chem. Prod. Res. Div.* **1986**, *25*, 179.

(46) Janssen, F. J. J. G.; van den Kerkhof, F. M. G.; Bosch, H.; Ross, J. R. H. *J. Phys. Chem.* **1987**, *91*, 6633.

(47) Busca, G. *Appl. Catal.*, in press.

(48) Gasior, M.; Haber, J.; Machej, T.; Czeppe, T. *J. Mol. Catal.* **1988**, *43*, 359.

(49) Chen, J. P.; Yang, R. T. *J. Catal.* **1990**, *125*, 411.

(50) Miyata, H.; Fujii, K.; Ono, T. *J. Chem. Soc., Faraday Trans. 1* **1988**, *84*, 3121.

(51) Okazaki, S.; Knurnasaka, M.; Yoshida, J.; Kosaka, K. *Ind. Eng. Chem. Prod. Res. Div.* **1981**, *20*, 301.

(52) Vuurman, M. A.; Wachs, I. E., to be published.

XPS. The Raman spectra reveal that the molecular structure of the vanadium oxide species in V_2O_5/TiO_2 is dependent on the surface coverage and surface hydration. At low vanadium oxide loading, hydrated tetrahedrally coordinated metavanadate species is favored under ambient conditions. Distorted octahedral vanadia is observed at moderate loadings which best match the hydrated decavanadate cluster. Under dehydrated conditions the metavanadate and decavanadate species are converted into two types of surface vanadium oxide species, a highly distorted coordinated species and a moderately distorted vanadium oxide species, the ratio of which is a function of the vandia coverage. The highly distorted vanadium oxide has a tetrahedral coordination and possesses one short $V=O$ bond and three bridging $V-O$ bonds to the support. For the moderately distorted species two structures have been proposed, both possessing a tetrahedrally coordination. Above monolayer coverage (>6%) crystalline V_2O_5 is also present on the titania surface. The WO_3/TiO_2 system shows the same structural dependence under ambient conditions with loading. At low tungsten oxide loading, tetrahedrally coordinated tungsten oxide (WO_4^{2-}) is observed while an octahedrally coordinated polytungstate species is formed at moderate loadings. Dehydration converts all the two-dimensional tungsten oxide species into a distorted octahedral coordinated structure, which possesses one short $W=O$ bond, one long opposing $W-O$ bond and four bridging $W-O$ bonds. Above 8%, the monolayer has been ex-

ceeded and crystalline WO_3 is also formed on the surface. The molecular structure of the mixed $V_2O_5-WO_3/TiO_2$ samples are not influenced by the sequence of impregnation with the starting materials. Under hydrated conditions, the metavanadate species, present at low vanadium oxide loading, are converted into a decavanadate species due to the acidic nature of tungsten oxide species. The decavanadate species, present at moderate vanadium oxide loadings, are found to be stable up to high tungsten oxide loadings. These situations occur because the hydrated metal oxide molecular structures are only dependent on the net pH at pzc. Crystalline V_2O_5 and crystalline WO_3 are not influenced by the presence of the other metal oxide. This is in agreement with the XPS data which suggest that the dispersion of both metal oxides is not influenced by the presence of the second metal oxide. Under dehydrated conditions, both the highly distorted vanadium oxide species and octahedrally coordinated tungsten oxide species are found to be present on the titania surface at all loadings and do not seem to be influenced by each other. The only influence observed in this study is that the moderately distorted vanadium oxide species become more abundant in the presence of surface tungsten oxide.

Colloid Particle Charge Determination via the Structure Factor $S(Q)$

H. Versmold,* U. Wittig, and W. Härtl

Institut für Physikalische Chemie, RWTH, D-5100 Aachen, F.R.G (Received: December 11, 1990)

The dependence of the structure factor $S(Q)$ of fluidlike ordered polymer colloid suspensions on ionic strength is investigated. It is found that a given amount of NaCl influences the structure much more than the same amount of NaOH. This behavior is explained in terms of an ion-exchange mechanism that takes place with NaOH but not with NaCl. By comparing the structure factor $S(Q)$ of samples titrated with NaOH with the $S(Q)$ of samples titrated with NaCl, one can determine the charge of the latex particles, if it is assumed that equal structure factors are due to equal ionic strength in corresponding suspensions.

Introduction

Considerable effort has been directed toward the understanding of the self-organization of supermolecular systems to form fluid-, glass-, and crystallike states.[1-3] Besides phenomenological and technological interest, the ultimate goal of such investigations is the understanding of the self-organization in terms of the interactions and properties of the constituents, from which the structure is formed.

In order to understand the structure of charge-stabilized systems from first principles, one should start with the determination of the particle charge. Next, statistical-mechanical methods would be necessary to determine the effective pair potential of mean force $V(r)$. Finally, statistical mechanics or computer simulation techniques could be used to predict the resulting structures. Despite the simplicity of this concept, each of the steps mentioned above is faced with severe difficulties.[3]

In this paper we focus on the problem of how the charge of colloid particles can be determined experimentally. Various physicochemical methods are presently used to determine the charge of polymer latex particles like conductometric titration,[4-6]

conductivity measurements,[7] and electrophoretic mobility.[8] In the context of the present investigation, conductometric titration is of particular interest, since it shows an interesting behavior, which initiated the present investigation.

For conductometric titrations the particles are usually cleaned and transferred into the protonated form by means of ion-exchange resins.[4] Thus, at the beginning of a titration experiment a high conductivity due to the H^+ counterions of the colloid particles is expected. By titration with NaOH, the conductivity should decrease until the equivalence point is reached since the highly mobile H^+ ions are replaced by Na^+ ions. Experiments show, however, that this simple concept does not work. Titration of a perfectly cleaned and protonated suspension with NaOH shows surprisingly little decrease of the conductivity.[5] Similarly, on addition of $Ba(OH)_2$ the conductivity starts to decrease significantly only as the equivalence point is approached.[4] The explanation of this behavior is that the protons in the diffuse double layer of the

(1) Safran, S. A.; Clark, N. A., Eds. *Physics of Complex and Supermolecular Fluids*; Wiley: New York, 1987.

(2) Pieranski, P. *Contemp. Phys.* **1983**, *24*, 25.

(3) Pusey, P. N. In *Liquids, Freezing and the Glass Transition*; Levesque, D., Hansen, J.-P., Zinn-Justin, J., Eds.; Elsevier: Amsterdam, preprint.

(4) Vanderhoff, J. W.; Van den Hul, H. J.; Tansk, R. J. M.; Overbeek, J. Th. G. In *Clean Surfaces: Their Preperation and Characterization for Interfacial Studies*; Goldfinger, G., Ed.; Marcel Dekker: New York, 1970.

(5) Labib, M.; Robertson, A. J. *J. Colloid Interface Sci.* **1980**, *77*, 154.

(6) Bangs, L. B. *Uniform Latex Particles*; Seragen: Indianapolis, 1984.

(7) Schaefer, D. W. *J. Chem. Phys.* **1977**, *66*, 3980.

(8) Hunter, R. J. *Zeta Potential in Colloid Science*; Academic Press: London, 1981.